Vol. 46 — N° 4 12 22 p. 825–836

GEOSTANDARDS and GEOANALYTICAL RESEARCH

Stable Neodymium Isotope Ratios of Geological Reference Materials

Jianghao **Bai** (1, 2, 3), Jinlong **Ma** (1, 2)*, Gangjian **Wei** (1, 2, 4), Le **Zhang** (1, 2), Chengshuai **Liu** (5, 6), Ting **Gao** (6), Yuhui **Liu** (3, 6) and Yufei **Liu** (7)

(1) State Key Laboratory of Isotope Geochemistry, Guangzhou Institute of Geochemistry, Chinese Academy of Sciences, Guangzhou 510640, China
(2) CAS Centre for Excellence in Deep Earth Science, Guangzhou 510640, China
(3) University of Chinese Academy of Sciences, Beijing 100049, China
(4) Southern Marine Science and Engineering Guangdong Laboratory, Guangzhou 511458, China
(5) Guangdong Key Laboratory of Agricultural Environment Pollution Integrated Control, Guangdong Institute of Eco-Environmental and Soil Sciences, Guangzhou 510650, China
(6) State Key Laboratory of Environmental Geochemistry, Institute of Geochemistry, Chinese Academy of Sciences, Guiyang 550081, China
(7) Guangzhou Marine Geological Survey, China Geological Survey, Guangzhou 510075, China
* Corresponding author E-mail: jlma@gig.ac.cn

Here, we report the stable Nd isotopic compositions of twenty-seven widely available geological reference materials (RMs) including silicates, sediments, soils and carbonates. Nd was purified from geological samples using a single TODGA resin column. The Nd isotopic ratios were determined via MC-ICP-MS using the combined standard-sample bracketing and internal normalisation method. The (long-term) intermediate measurement precision of $\delta^{146/144}$Nd values relative to the reference material JNdi-1 was greater than 0.030‰ (2*s*). Measurements of five previously analysed RMs yielded $\delta^{146/144}$Nd values that were consistent with those obtained using the double-spike method. The igneous rocks showed minimal variations in their $\delta^{146/144}$Nd values, which ranged from -0.039‰ to +0.015‰. The sediments displayed large stable Nd isotopic fractionations ranging from -0.099‰ to +0.057‰, implying differences in their sources. The soil RMs showed a range of -0.093‰ to -0.010‰, likely owing to complex geological processes such as the degree of chemical weathering. The sedimentary rock dolomite had the heaviest $\delta^{146/144}$Nd values at +0.147 ± 0.032‰ (2*s*, *n* = 3). Of the analysed RMs, the $\delta^{146/144}$Nd values of thirteen of them are being reported for the first time. The datasets presented here should play fundamental role in quality assurance and allow for universal comparisons for stable Nd isotope systematics.

Keywords: stable Nd isotopic ratio, TODGA resin column, C-SSBIN, MC-ICP-MS, geological reference materials.

Received 22 Oct 21 – Accepted 23 Jun 22

Neodymium is a moderately to highly incompatible, non-conservative, and highly refractory rare earth element (REE). It contains two radiogenic isotopes (^{142}Nd and ^{143}Nd) and five stable isotopes (^{144}Nd, ^{145}Nd, ^{146}Nd, ^{148}Nd and ^{150}Nd). The stable Nd isotope ratio (^{146}Nd/^{144}Nd) is a recently proposed metric and is commonly reported as relative to that of the reference material JNdi-1:

$$\delta^{146/144}\mathrm{Nd}_{\underline{JNdi-1}} = \left[\frac{\left(^{146}\mathrm{Nd}/^{144}\mathrm{Nd}_{\mathrm{sample}}\right)}{\left(^{146}\mathrm{Nd}/^{144}\mathrm{Nd}_{\mathrm{JNdi-1}}\right)}\right] - 1 \quad (1)$$

Initial works by Wakaki and Tanaka (2012) reported an analysis protocol for stable Nd isotopes using the double-spike thermal ionisation mass spectrometry (DS-TIMS) technique; they observed significant stable Nd isotopic variations of up to 1.404‰ during cation exchange column chromatography and investigated stable Nd isotope data for ten commercial Nd oxide reagents and La Jolla Nd. To date, the most stable data for natural samples have been obtained using DS-TIMS (McCoy-West *et al.* 2017, 2020a, 2020b, 2021, 2022). McCoy-West *et al.* (2017) were the first to present comprehensive stable Nd isotope data for chondritic meteorites and terrestrial rocks using this technique. They found that the three types of chondritic meteorites, namely, carbonaceous, enstatite, and ordinary chondrites, all have broadly similar stable Nd isotopic ratios, exhibiting overall chondritic

doi: 10.1111/ggr.12451

mean values of $\delta^{146/144}$Nd = -0.025 ± 0.025‰ (2*s*, *n* = 39), which was subsequently recalculated to be -0.027 ± 0.026‰ (2*s*, *n* = 39) by McCoy-West *et al.* (2020a). Terrestrial samples also exhibit similar stable Nd isotopic compositions, showing a mean value for the bulk silicate Earth (BSE) of $\delta^{146/144}$Nd = -0.022 ± 0.034‰ (2*s*, *n* = 30) which was redefined by McCoy-West *et al.* (2021) to $\delta^{146/144}$Nd = -0.024 ± 0.031‰ (2*s*, *n* = 80) based on a global compilation of mid-ocean ridge, ocean island, continental intraplate, and island arc basalts. When using a DS-TIMS technique there is no imperative to obtain 100% yield and achieve perfect separation of Nd from Ce and Sm, but the calculations are complicated. Several studies have attempted to develop stable Nd isotope analytical procedures using multi-collector inductively coupled plasma-mass spectrometry (MC-ICP-MS), because it is easy to perform and is sufficiently precise to account for the natural variations (Ma *et al.* 2013, Ohno and Hirata 2013, Saji *et al.* 2016, Bothamy and Galy 2021). However, perfect Ce–Pr–Nd separations with 100% Nd yields are required when not using a double spike during measurements. Wang *et al.* (2017) and Bai *et al.* (2021) achieved this using a single-step TODGA resin column and analysed the stable Nd isotopes in geological samples. Therefore, stable Nd isotopes are being developed for use in many fields and applications, such as magmatic evolution (McCoy-West *et al.* 2017, 2020b, 2021, 2022), sediment provenance (Liu et al. 2018), and anthropogenic pollution evaluation (Bothamy and Galy 2021). The currently available data is approximately 0.25‰ in natural samples (Ma *et al.* 2013, McCoy-West *et al.* 2017, 2020a, 2020b, 2021, 2022, Liu *et al.* 2018), which means that it may provide a new geochemical signature for a diverse range of geological processes such as planetary differentiation, global Nd circulation, petrogenetic, and deposit studies.

The applicability of stable Nd isotope is based on the precise and accurate determination of its isotopic compositions. Geochemical reference materials (RMs) play a fundamental role in theses analyses, which include evaluating the possibility of chromatographic separation, mass spectrometry, and comparing the $\delta^{146/144}$Nd values obtained from different laboratories (e.g., He *et al.* 2015, Teng *et al.* 2015, Zhao *et al.* 2016, Feng *et al.* 2017, An *et al.* 2019, Nakada *et al.* 2019, Zhu *et al.* 2021). However, stable Nd isotopic data for geological RMs are scarce, and most of the samples studied are igneous rocks, particularly basaltic rocks (Ma *et al.* 2013, Saji *et al.* 2016, McCoy-West *et al.* 2017, 2020a, 2020b, 2021, 2022, Wang *et al.* 2017, Bai *et al.* 2021). In fact, the $\delta^{146/144}$Nd values of soils, sediments and sedimentary rocks have rarely been reported. However, such data are essential for avoiding analytical artefacts and improving our understanding of global Nd cycles.

In this study, a set of commonly used and commercially available geological RMs, including thirteen igneous rocks, nine stream/marine sediments, four soils and one sedimentary rock, were measured using a Neptune Plus MC-ICP-MS. These RMs cover a wide gamut of compositions, with their SiO_2 mass fractions ranging from 0.21% to 76.8% *m/m*, MgO mass fractions from 0.04% to 17.82% *m/m*, and Nd mass fractions from 5.3 to 247 μg g^{-1}. This study provides new stable Nd isotopic data for a series of RMs and builds a useful database for stable Nd isotope geochemistry.

Sample preparation, column chemistry and instrumental analysis

Detailed procedures for sample preparation, column chemistry, and the instrumental analysis of stable Nd isotopes have been reported by Bai *et al.* (2021). High purity acids (HCl, HNO_3 and HF) were produced by sub-boiling distillation using a Savillex DST-1000 system (USA). Ultra-pure water (resistivity: 18.2 MΩ cm) was obtained using an ion-exchange water purification system (Millipore, USA). Pure Eu single-element solutions (1000 μg g^{-1}) and optimal-grade H_2O_2 were purchased from the Beijing General Research Institute for Nonferrous Metals and Thermo Fisher Scientific, respectively. The 2 ml of TODGA resin (Eichrom, USA) with 50–100 μm particle size was packed in an exchange column (0.7 cm ID × 9 cm total length) manufactured by the Triskem Company.

Reference materials with a wide range of matrices and chemical compositions were acquired from the United States Geological Survey (USGS), Geological Society of Japan (GSJ), and National Research Centre for Geoanalysis, China (NRCG). These included basalts, andesites, granodiorites, diabases, granites, rhyolites, sediments, polymetallic nodules, marine sediments, stream sediments, soils, and dolomites. Detailed information on the samples, including the rocks type, provider, actual mass of each dissolved sample that was dissolved, mass fractions of major elements, and loss-on-ignition (LOI) values are listed in online supporting information Table S1.

The samples were dissolved in a class 100 hood at the Guangdong Key Laboratory of Agricultural Environment Pollution Integrated Control, Guangdong Institute of Eco-Environmental and Soil Sciences. Approximately 10–80 mg of the sample powders, including 1 μg of Nd, were weighed into 15 ml PFA Savillex beakers. The actual mass of each dissolved sample is shown in Table S1. For silicate samples, the whole-rock powders were dissolved in a mixture of concentrated HF and HNO_3 (3,1) for 7 days on a hot plate at 120 °C. Once in solution form, the samples were

evaporated to dryness at 100 °C and redissolved in *aqua regia*, and then 2 ml of 6 mol l^{-1} HCl twice to remove the fluorides. For the sediments and soil samples, aqua regia and H_2O_2 were used repeatedly until all the organic matter had been decomposed. After that, the samples were digested with a 3:1 mixture of concentrated HF and HNO_3 in capped beakers at 120 °C. Subsequently, they were evaporated to dryness and redissolved in 6 mol l^{-1} HCl for at least 24 h. Because JDo-1 has low Nd mass fractions, three aliquots of JDo-1 were decomposed separately. Dilute HCl was added drop wise to remove CO^{2-}_3 and then evaporated to dryness. The remaining residues, along with the silicates, were treated with concentrated HF and HNO_3 and subsequently with 6 mol l^{-1} HCl. Finally, 1 ml of concentrated HNO_3 was added twice to all the completely digested samples, which were then dissolved in 0.5 ml of 2 mol l^{-1} HNO_3 for chromatographic column separation.

Neodymium was separated using an exchange column filled with 2 ml TODGA resin purchased from Eichrom industry. The pre-cleaned column was further cleaned thrice using 5 ml of 8 mol l^{-1} HNO_3 and 5 ml of 0.1 mol l^{-1} HCl alternately. Then, the column was conditioned with 6ml of 2 mol l^{-1} HNO_3. Next, 0.5 ml of a pre-prepared 2 mol l^{-1} HNO_3 solution containing 1 μg Nd was loaded into the column. Subsequently, another 4.5 ml of 2 mol l^{-1} HNO_3 was added into the column to leach the matrix elements, such as Na, Mg, Al, Ti, Ba, Fe, Mn, K, and Rb. Pb, Sr and Ca were eluted using 15 ml of 8 mol l^{-1} HNO_3. Afterwards, 26 ml of 2.6 mol l^{-1} HCl was used to remove La, Ce and Pr, and 12 ml of 2 mol l^{-1} HCl was used to collect Nd. The purified Nd samples were dried and treated with concentrated HNO_3 once. Finally, the purified Nd portion was redissolved in 2% HNO_3 and diluted to 100 ng g^{-1} to examine the matrix/Nd ratios, in particular Sm/Nd ratio, and the yield of Nd, using ICP-MS. No significant effects of the matrix elements such as Ca and isobaric elements such as Sm in the analyte solution were observed during ICP-MS (Table S2). Otherwise, a second pass though the column is necessary. The yield of Nd purification process was greater than 99%, which were calculated based on the Nd mass fractions in the collected Nd cuts relative to the total Nd loading amount (Table S2).

The Nd isotopic ratios were determined using a Thermo-Fisher Scientific Neptune Plus MC-ICP-MS at the State Key Laboratory of Isotope Geochemistry (SKLaBIG), Guangzhou Institute of Geochemistry, Chinese Academy of Sciences (GIG-CAS). The instrument used is a double-focus mass spectrometer equipped with nine Faraday cups and four ion counters. ^{140}Ce, ^{142}Nd, ^{143}Nd, ^{144}Nd, ^{145}Nd, ^{146}Nd, ^{151}Eu and ^{153}Eu were collected simultaneously in Faraday cups L4, L3, L2, L1, C, H1, H2, and H3, respectively. ^{140}Ce was monitored to calculate the isobaric interferences of ^{142}Ce on ^{142}Nd using ^{142}Ce = 0.12589 × ^{140}Ce (Willig and Stracke 2018). In theory, the signals of ^{147}Sm should also be collected to monitor the isobaric interferences of ^{144}Sm on ^{144}Nd. However, two of the high-Faraday cups, H3 and H4, were mounted together, and two ion counters were assigned between H3 and H4 in our instrument. Cup H4 did not reach to the position of *m/z* 153(^{153}Eu) when H3 was at the position of *m/z* 151(^{151}Eu). To determine the ratio of ^{153}Eu/^{151}Eu, we therefore gave up to measure ^{147}Sm because Sm could be removed completely from Nd in our column chemistry (see Figure 1 in Bai *et al.* (2021)). All the samples analysed here had a Sm/Nd ratio of less than 0.000080 (Table S2), with the ^{144}Sm/^{144}Nd ratio being 0.000010, and an overall variation in the $\delta^{146/144}$Nd of 0.010‰, which could be ignored at our current level of precision (0.030δ). In fact, Ohno and Hirata (2013) demonstrated that the stable Nd isotopic measurements were valid when the purified Nd samples have a Sm/Nd ratio of less than 0.001. Combined standard-sampled bracketing and Eu internal normalisation correction model was used to correct instrumental mass discrimination. Sample solutions in 2% HNO_3 were introduced into the plasma using a self-aspiration capillary PFA nebuliser (50 μl min^{-1}) and a dual cyclonic-Scott spray chamber. All the measurements were performed in the static mode with a low mass resolution. Before the measurements, all the samples to be introduced into the instruments were carefully adjusted such that the differences with respect to a mixed solution of JNdi-1 and Eu single-element solution, which contained 200 ng g^{-1} Nd and 48 ng g^{-1} Eu, respectively (typically corresponding to 17.5 V per μg g^{-1} of ^{144}Nd and 37.0 V per μg g^{-1} of ^{153}Eu, respectively), were within 10%. The background signal of 2% HNO_3 for ^{144}Nd signal was less than 0.2 mV.

Results

The stable Nd isotopic ratios of the twenty-seven geological RMs analysed in this study are listed in Table 1. The listed $\delta^{146/144}$Nd value for each RM is the mean of at least three repeated measurements. Moreover, the stable Nd isotopic compositions of thirteen of the twenty-seven RMs are being reported for the first time. Overall, the Nd isotopic ratios of the twenty-seven geological RMs ranged from -0.099 ± 0.019‰ (2*s*, *n* = 3) in a marine sediment RM (GBW07335) to +0.147 ± 0.032‰ (2*s*, *n* = 3) in a dolomite (JDo-1) (see Table 1 and Figure 1). The greatest range of $\delta^{146/144}$Nd value reached 0.246‰ in actual samples, eight times greater than our "external" precision of ±0.030‰ (2*s*).

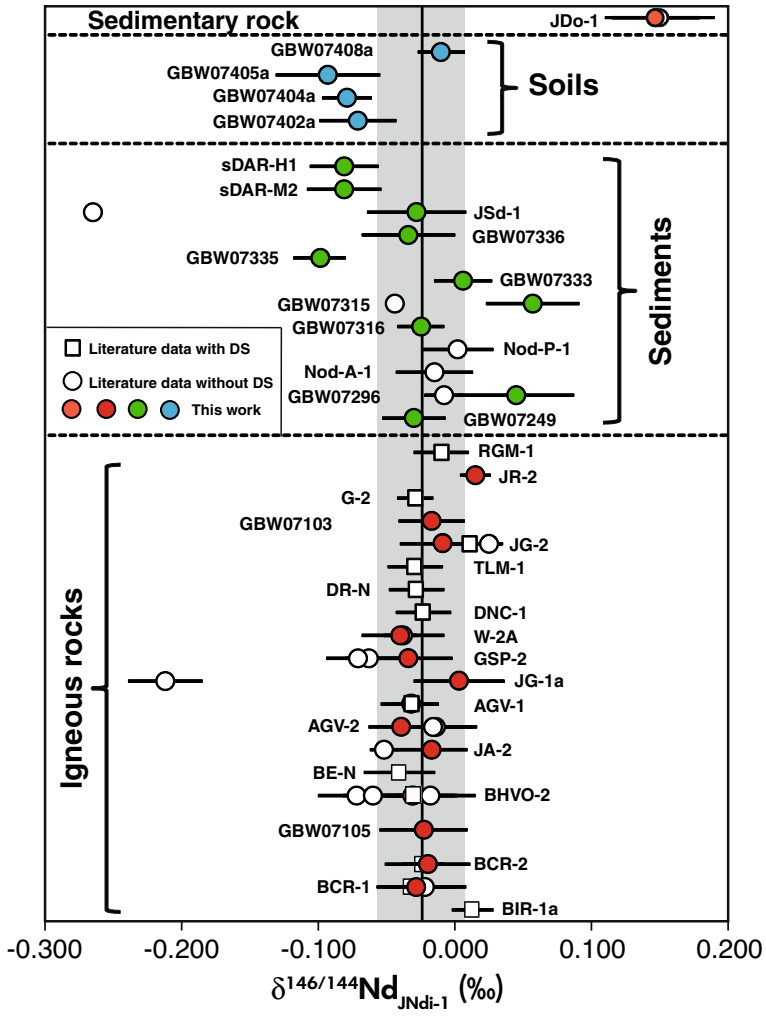

Figure 1. Comparison of $\delta^{146/144}$Nd values measured in this study with those reported in literature data. Vertical grey area represents $\delta^{146/144}$Nd value of BSE, which is -0.024 ± 0.031‰ (2*s*, *n* = 80) taken from McCoy-West *et al.* (2021). Filled brown, red, green, and blue circles represent stable Nd isotopic compositions measured in this study, while the open circles and squares represent the literature data with double spike (DS) and without double spike, respectively, summarised in Table 1. Range bars represent two standard deviations (2*s*).

The $\delta^{146/144}$Nd values for basaltic to dacitic igneous rocks showed only small variations, with the mean value being -0.026 ± 0.020‰ (2*s*, *n* = 9), which is identical to that of estimated the bulk silicate Earth (BSE) (-0.024 ± 0.031‰, 2*s*, *n* = 80, McCoy-West *et al.* 2021) and chondrites (-0.027 ± 0.026‰, 2*s*, *n* = 39, McCoy-West *et al.* 2017, 2020a). The four felsic igneous rocks (> 70% *m/m* SiO_2) exhibited slightly larger $\delta^{146/144}$Nd values at -0.002 ± 0.028‰ (2*s*, *n* = 4). The stream and marine sediments also showed heterogeneity in their $\delta^{146/144}$Nd values, which ranged from -0.099 ± 0.019‰ (2*s*, *n* = 3) in GBW07335 to +0.057 ± 0.034‰ (2*s*, *n* = 3) in GBW07315. The soil samples yielded $\delta^{146/144}$Nd values ranging from -0.093 ± 0.038‰ (2*s*, *n* = 3) in GBW07405a to -0.010 ± 0.017‰ (2*s*, *n* = 3) in GBW07408a. The JDo-1, a dolomite RM, had the heaviest $\delta^{146/144}$Nd value of +0.147 ± 0.032‰ (2*s*, *n* = 3).

Discussion

The stable Nd isotopic compositions of the twenty-seven geological RMs investigated in this study as well as those reported previously are listed in Table 1. Based on the rock type, the RMs can be divided into four groups. Group I consists of igneous rocks including basalt, andesite, granodiorite, diabase, dolerite, tonalite, granite, and rhyolite. Group II is composed of polymetallic nodule, stream, and marine sediments. Group III is soil RMs. Group IV is a dolomite. Stable Nd isotopic variations were observed in

Table 1.
Stable Nd isotopic composition of reference materials from this work and the literature

Group	RM	SiO_2 (% *m/m*)[a]	MgO (% *m/m*)[a]	CIA[b]	Nd ($\mu g\ g^{-1}$)[b]	$\delta^{146}Nd$ (‰)	2*s*[c]	*n*[d]	Reference [e]
Pure Nd standard solutions	JNdi-1					0.000	0.030	50	This work
						0.000	0.027	210	Bai *et al.* (2021), C-SSBIN
	Nd-GIG					0.221	0.029	8	This work
						0.226	0.021	20	Bai *et al.* (2021), C-SSBIN
Igneous rock (Group I)	BIR-1	47.2	9.5	50.4	2.5	0.013	0.015	8	McCoy-West *et al.* (2020a), ^{145}Nd-^{150}Nd
	BCR-1	54.5	3.5	53.0	28.3	-0.028	0.029	3	This work
						-0.022	0.030	4	Bai *et al.* (2021), C-SSBIN
						-0.031	0.021	3	McCoy-West *et al.* (2017)[g], ^{145}Nd-^{150}Nd
						-0.031	0.015	5	McCoy-West *et al.* (2021a), ^{145}Nd-^{150}Nd
	BCR-2	54.1	3.6	52.8	29.3	-0.020	-0.031	3	This work
						-0.023	0.015	2	McCoy-West *et al.* (2021a), ^{145}Nd-^{150}Nd
	GBW07105	44.6	7.8	48.0	54.0	-0.023	0.032	3	This work
	BHVO-2	49.8	7.2	48.7	24.7	-0.031	0.033	3	This work
	BHVO-2-R[f]					-0.035		1	This work
						-0.030	0.030	4	Bai *et al.* (2021), C-SSBIN
						-0.030	0.014	6	McCoy-West *et al.* (2020a), ^{145}Nd-^{150}Nd
						-0.018	0.033	21	Wang *et al.* (2017), SSB
						-0.072	0.010	5	Ma *et al.* (2013), SSB
						-0.060	0.040	5	Saji *et al.* (2016), SSB
	BE-N	38.2	13.1	35.0	66.5	-0.037	0.024	5	McCoy-West *et al.* (2017)[g], ^{145}Nd-^{150}Nd
	JA-2	56.3	7.7	58.0	14.0	-0.017	0.026	3	This work
						-0.052	0.010	1	Ma *et al.* (2013), SSB
	AGV-2	59.2	1.8	58.1	30.9	-0.039	0.024	3	This work
						-0.014	0.030	4	Bai *et al.* (2021), C-SSBIN
						-0.016	0.029	20	Wang *et al.* (2017), SSB
	AGV-1	59.4	1.5	58.6	32.1	-0.033	0.021	3	This work
						-0.033	0.008	3	McCoy-West *et al.* (2017)[g], ^{145}Nd-^{150}Nd
	JG-1a	72.2	0.7	59.9	20.5	0.003	0.033	3	This work
						-0.212	0.027	3	Ma *et al.* (2013), SSB
	GSP-2	66.6	1.0	59.2	200.0	-0.034	0.032	3	This work
						-0.063	0.031	4	Bai *et al.* (2021), C-SSBIN
						-0.071	0.009	2	Ma *et al.* (2013), SSB
	W-2A	52.1	6.4	50.2	12.8	-0.038	-0.030	3	This work
						-0.040	0.012	5	Saji *et al.* (2016), SSB
	DNC-1	47.1	10.1	57.8	5.7	-0.025	0.020	1	McCoy-West *et al.* (2017)[g], ^{145}Nd-^{150}Nd
	DR-N	52.9	4.4	59.9	23.5	-0.034	0.010	2	McCoy-West *et al.* (2017)[g], ^{145}Nd-^{150}Nd
	TLM-1	58.7	3.3	61.0	17.5	-0.032	0.020	1	McCoy-West *et al.* (2017)[g], ^{145}Nd-^{150}Nd
	JG-2	76.8	0.0	58.1	26.0	-0.009	0.031	3	This work
						0.010	0.004	2	McCoy-West *et al.* (2017)[g], ^{145}Nd-^{150}Nd
						0.025	0.010		Ma *et al.* (2013), SSB
	GBW07103	72.8	0.4	58.0	47.0	-0.017	0.024	3	This work
	G-2	68.9	0.8	59.4	54.4	-0.029	0.013	7	McCoy-West *et al.* (2020a), ^{145}Nd-^{150}Nd
	JR-2	75.7	0.0	58.9	20.7	0.015	0.011	3	This work
	RGM-1	73.1	0.3	59.1	19.2	-0.010	0.007	2	McCoy-West *et al.* (2017)[g], ^{145}Nd-^{150}Nd

Table 1 (continued).
Stable Nd isotopic composition of reference materials from this work and the literature

Group	RM	SiO_2 (% *m/m*)[a]	MgO (% *m/m*)[a]	CIA[b]	Nd ($\mu g\ g^{-1}$)[b]	$\delta^{146}Nd$ (‰)	2*s*[c]	*n*[d]	Reference [e]
Sediments (Group II)	GBW07249	13.3	2.0	39.0	247.0	-0.030	0.023	4	Bai *et al.* (2021), C-SSBIN
	GBW07296	12.3	3.6	42.3	121.0	0.045	0.042	3	This work
						-0.008	0.014	2	Ma *et al.* (2013), SSB
	Nod-A-1	3.8	4.8	18.5	94.0	-0.015	0.028	4	Bai *et al.* (2021), C-SSBIN
	Nod-P-1	13.9	3.3	42.5	120.0	0.002	0.026	4	Bai *et al.* (2021), C-SSBIN
	GBW07316	31.6	2.0	21.6	51.0	-0.025	0.017	4	This work
	GBW07315	51.1	3.0	47.7	75.0	0.057	0.034	3	This work
						-0.044			Ma *et al.* (2013), SSB
	GBW07333	54.0	3.1	68.7	33.1	0.006	0.021	3	This work
	GBW07335	59.6	2.5	57.2	32.6	-0.099	0.019	3	This work
	GBW07336	44.9	2.2	40.5	26.0	-0.034	0.034	3	This work
	JSd-1	66.5	1.9	64.8	17.7	-0.028	0.036	3	This work
						-0.265		1	Ma *et al.* (2013), SSB
	sDAR-M2	73.5	0.5	73.0	39.7	-0.081	0.027	3	This work
	sDAR-H1	65.5	1.3	66.6	36.2	-0.081	0.025	3	This work
Soil (Group III)	GBW07402a	66.0	1.4	55.8	55.0	-0.071	0.028	3	This work
	GBW07404a	51.0	0.5	94.4	40.0	-0.079	0.018	3	This work
	GBW07405a	61.5	0.7	92.7	27.0	-0.093	0.038	3	This work
	GBW07405a-R[f]					-0.082		1	This work
	GBW07408a	60.1	2.0	50.3	31.0	-0.010	0.017	3	This work
Sedimentary rock (Group IV)	JDo-1	0.2	17.8	0.0	5.3	0.147	0.032	3	This work
						0.150	0.040		Ohno and Hirata (2013)

[a] The SiO_2,MgO,and Nd mass fractions of reference materials are taken from http://georem.mpch-mainz.gwdg.de/
[b] CIA=$Al_2O_3/(Al_2O_3+CaO^*+Na_2O+K_2O)$, CaO^* represents the fraction of CaO in silicate. The data were taken from Table S1.
[c] 2*s* 2 standard deviation.
[d] a duplicate analysis number of the same solution.
[e] C-SSBIN, combined standard sample bracketing and internal normalisation. SSB, standard sample bracketing; ^{145}Nd-^{150}Nd, ^{145}Nd-^{150}Nd double spike.
[f] full-procedure duplicate
[g] Data from McCoy-West *et al.* (2017) are recalculated (see the appendix of McCoy-West *et al.* 2020a)

theses RMs, which can be used as potential indicators for various geological processes. In the following sections, we first describe the evaluation results of the quality of the data on these RMs and then explore the stable Nd isotopic behaviours from high-temperature magmatic evolution to low-temperature chemical weathering.

Data quality

The stable Nd isotopic ratios for pure Nd reference solutions and well-studied geological RMs are listed in Table 1. The repeat analyses of the reference material JNdi-1 and our laboratory in-house Nd-GIG allowed for the evaluation of the long-term stability of the instrument used. The results indicated that the reference materials JNdi-1 and Nd-GIG produced total mean $\delta^{146/144}Nd$ values of 0.000 ± 0.031‰ (2*s*, *n* = 50) and + 0.221 ± 0.029‰ (2*s*, *n* = 8) (Table 1), respectively. They both show a small variation within uncertainty of the previous determinations reported in Bai *et al.* (2021) (Figure 2). Three rock types, BHVO-2, AGV-2 and GSP-2, were digested seven to ten times and processed through chemistry and analysed separately (Table 2 and Figure 3). The results suggested that the "external" precision for the three rocks was better than ±0.030‰. The analyses of BCR-1, BCR-2, BHVO-2, AGV-1 and JG-2, which have been studied well, yielded mean $\delta^{146/144}Nd$ values of -0.028 ± 0.029 ‰ (2*s*, *n* = 3), -0.020 ± 0.031‰ (2*s*, *n* = 3), -0.031 ± 0.033‰ (2*s*, *n* = 3), -0.033 ± 0.021‰ (2*s*, *n* = 3) and -0.009 ± 0.031‰ (2*s*, *n* = 3) respectively, these were in excellent agreement with the data published based on the DS-TIMS methodology (McCoy-West *et al.* 2017, 2020a, 2021), thereby confirming the reliability of the data obtained in this study (Figure 1). The three whole-procedure blanks were 0.02, 0.06 and 0.31 ng, which were negligible compared with Nd loading amount of 1 μg. The Nd recovery was above 99% (Table S2). Overall, the results of the tests performed on the pure Nd reference solutions and well-studied geological RMs demonstrated that stable Nd isotopic ratios could be accurately measured in this study.

Group I: Igneous rocks

The results for the thirteen igneous rocks combined with earlier studies, including six basalts, three andesites, two granodiorites, one diabase, two dolerites, one tonalite are listed in Table 1. As shown in this table, the different sets of powders of the basaltic to dacitic RMs, such as BHOV-2, AGV-2 and W-2A, gave identical stable Nd isotopic

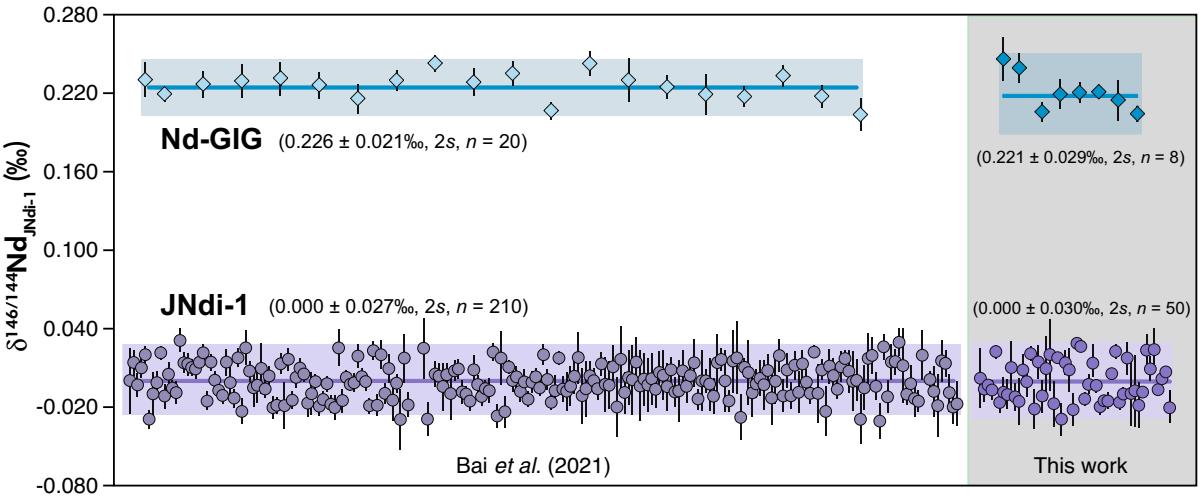

Figure 2. Intermediate meaurement precision of reference materials JNdi-1 and Nd-GIG measured using Neptune Plus MC-ICP-MS instrument at GIG-CAS. Light green data points are from Bai *et al.* (2021) and dark green data points were analysed in this study. Circles represent JNdi-1, diamonds represent Nd-GIG. No long-term $\delta^{146/144}$Nd drift was observed during measurements.

compositions of -0.026 ± 0.020‰ (2*s*, *n* = 9), this value is in good agreement with that estimated for BSE (-0.024 ± 0.031‰, 2*s*, *n* = 80, (McCoy-West *et al.* 2021)). The homogenous Nd isotopic compositions in the basaltic to dacitic rocks was the same indicated that no systematic changes occurred during general magmatic differentiations (Figure 4), similar to the case for other non-traditional stable isotopic systematics, such as Ca, Fe, Zr and Mo (He *et al.* 2015, Zhao *et al.* 2016, Feng *et al.* 2017, Liu *et al.* 2017, Inglis *et al.* 2019, McCoy-West *et al.* 2019). In contrast, the felsic rocks have slightly heavier $\delta^{146/144}$Nd values, which is likely attributable to the crystallisation of the accessory mineral phases such as monazite and apatite during late-stage granitic differentiation (McCoy-West *et al.* 2017, 2020a, b, 2021, 2022).

The $\delta^{146/144}$Nd data for the igneous rock RMs, excluding rock JG-1a, as measured in this study matched the mean values reported in the literature within the limits of uncertainty (see Table 1). The mean $\delta^{146/144}$Nd values obtained for JG-1a in this study were + 0.003 ± 0.033‰ (2*s*, *n* = 3), whereas -0.212 ± 0.027‰ (2*s*, *n* = 3) in Ma *et al.* (2013). The stable Sm isotopic composition of JG-1a was measured by Wakaki and Tanaka (2016), who reported only small variations. Considering that Nd and Sm have mutually similar geochemical behaviours, coordinated variation of their isotopic systematics would also be expected. As shown in Figure 5, the $\delta^{152/150}$Sm values of available RMs were strongly correlated with the $\delta^{146/144}$Nd values obtained in this study. Moreover, the Eu isotopic compositions of five of the twenty-seven RMs (BCR-2, BHVO-2, BIR-1, GSP-2 and JG-1a) measured by Lee and Tanaka (2019) did not also show apparent isotopic fractionation at their analytical precision level (0.08‰). This result implies that the basaltic to dacitic magma-forming processes probably do not also cause Eu isotopic fractionation, although Eu may occur the Eu(II)-Eu(III) exchange reaction. Thus, the relatively large discrepancy in JG-1a is probably attributable to the incomplete Nd yield during their Ce removal processes wherein the heavier isotope ^{146}Nd being preferentially lost, leading to the enrichment of the lighter isotope ^{144}Nd at the back boundary of their Nd cut (McCoy-West *et al.* 2017). This phenomenon has also been observed in the other isotopes, such as Sm, Eu and Ca, in previous studies (Wakaki and Tanaka 2012, 2016, Zhu *et al.* 2016, Lee and Tanaka 2019).

Group II: Sediments

To date, stable Nd isotopic data for sediments have rarely been reported. The available data on sediments were reported by Ma *et al.* (2013) and Bai *et al.* (2021). The results obtained in this study for the twelve sediments RMs along with those reported previously are shown in Table 1. The RMs included four polymetallic nodules, five marine sediments, one stream sediment, and two sediments, and yielded the $\delta^{146/144}$Nd values ranging from -0.099‰ to +0.057‰. The four polymetallic nodules (GBW07249, GBW07296, Nod-A-1, and Nod-P-1) yielded $\delta^{146/144}$Nd values ranging from -0.030‰ to +0.045‰, which are

Table 2.
Neodymium isotope ratio of the USGS RMs BHVO-2, AGV-2 and GSP-2

Sample	Date	Mass (g)	$\delta^{146/144}$Nd	SE	2*s*
BHVO-2-(1)	11-09-2020	0.04400	-0.032	0.012	
BHVO-2-(2)	21-06-2021	0.04231	-0.035	0.012	
BHVO-2-(3)	23-06-2021	0.04446	-0.035	0.017	
BHVO-2-(4)	14-10-2021	0.04857	-0.027	0.009	
BHVO-2-(5)	15-03-2022	0.04967	-0.054	0.001	
BHVO-2-(6)	15-03-2022	0.04755	-0.037	0.019	
BHVO-2-(7)	16-03-2022	0.04627	-0.010	0.011	
		MEAN	**-0.033**		**0.026**
AGV-2-(1)	12-09-2020	0.03770	-0.015	0.021	
AGV-2-(2)	21-06-2021	0.03270	-0.050	0.014	
AGV-2-(3)	15-10-2021	0.03378	-0.008	0.012	
AGV-2-(4)	16-02-2022	0.03180	-0.028	0.019	
AGV-2-(5)	15-03-2022	0.03328	-0.044	0.017	
AGV-2-(6)	15-03-2022	0.03928	-0.037	0.015	
AGV-2-(7)	15-03-2022	0.03350	-0.031	0.019	
AGV-2-(8)	16-03-2022	0.03486	-0.021	0.014	
AGV-2-(9)	16-03-2022	0.03133	-0.039	0.011	
AGV-2-(10)	16-03-2022	0.03589	-0.040	0.008	
		MEAN	**-0.031**		**0.026**
GSP-2-(1)	13-09-2020	0.00820	-0.068	0.013	
GSP-2-(2)	22-06-2021	0.01125	-0.037	0.018	
GSP-2-(3)	16-10-2021	0.00766	-0.025	0.011	
GSP-2-(4)	15-03-2022	0.00567	-0.042	0.018	
GSP-2-(5)	15-03-2022	0.00685	-0.024	0.014	
GSP-2-(6)	15-03-2022	0.00821	-0.037	0.019	
GSP-2-(7)	15-03-2022	0.00984	-0.016	0.015	
GSP-2-(8)	16-03-2022	0.00648	-0.021	0.014	
GSP-2-(9)	16-03-2022	0.00579	-0.032	0.015	
GSP-2-(10)	16-03-2022	0.00476	-0.025	0.015	
		MEAN	**-0.033**		**0.030**

Each analysis represents a separate measurement (n = 1); () is a separate digestion and processing through chemistry plus analysis

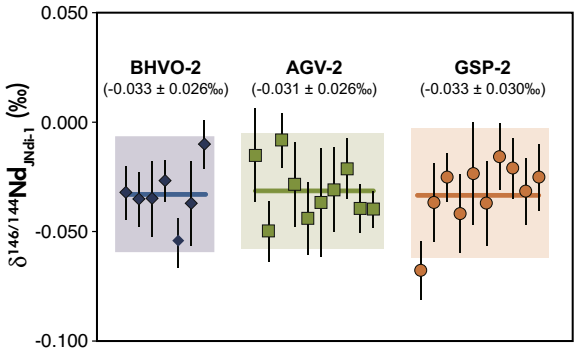

Figure 3. Intermediate measurement precision of the USGS geological reference materials BHVO-2, AGV-2 and GSP-2 after replicated digestion and processing through chemistry and being analysed separately. The complete dataset is shown in Table 2. Precision of $\delta^{146/144}$Nd values analysed here is better than ±0.030‰.

slightly different from the BSE value with $\delta^{146/144}$Nd = -0.024 ± 0.031‰ (2*s*, n = 80) (McCoy-West *et al.* 2017, 2020a, 2021). The five marine sediments (GBW07316, GBW07315, GBW07333, GBW07335 and GBW07336) showed highly variable $\delta^{146/144}$Nd signatures, with the values ranging from -0.099‰ to +0.057‰. The stream sediment JSd-1 had a $\delta^{146/144}$Nd value of -0.028 ± 0.036‰ (2*s*, n = 3), which is similar to that of igneous rocks. The remaining sediments showed $\delta^{146/144}$Nd values (-0.081 ± 0.027‰ (2*s*, n = 3) and -0.081 ± 0.025‰ (2*s*, n = 3)) similar to that of marine sediments GBW07335 and within the range of those of the sediment RMs. Interestingly, a rough negative relationship was observed between the $\delta^{146/144}$Nd and SiO_2 mass fractions (Figure 4a), and a positive one between MgO (Figure 4b) and Nd mass fractions (Figure 4c). These correlations suggest that the variations in the stable Nd isotopic ratios probably reflect the changes in the contributions of the different Nd sources. The $\delta^{146/144}$Nd value of JSd-1 (-0.265‰) as reported by Ma *et al.* (2013) showed large differences compared with that obtained in this study (-0.028 ± 0.036‰, (2*s*, n = 3)). Similar to the case for JG-1a, this result may be caused by an artificial isotope effect that occurs in their column chemistry.

Group III and IV: Soil and carbonate

The soil RMs measured in this study included a chestnut soil from Bayan Obo area, a limestone-forming soil from Yizhou, Guangxi Province, a yellow-red soil from the Qibaoshan polymetallic ore field, and a loess sample from Luochuan on the Loess Plateau, China. The $\delta^{146/144}$Nd values of these soil RMs ranged from -0.093‰ to -0.010‰, probably reflecting the effects of the climatic conditions, source compositions, or chemical processes. The chemical index of alteration (CIA), expressed as molar $A_2O_3/(A_2O_3 + CaO^* + Na_2O + K_2O)$ (where CaO* is the amount of CaO in the silicate phases), is a practical method for evaluating the effects of chemical weathering (Nesbitt and Young 1982). As illustrated in Figure 6, a roughly negative relationship was observed between the $\delta^{146/144}$Nd and CIA values of these RMs, including the soils. This suggests that the degree of chemical weathering degree is an important driving factor for the stable Nd isotopic variations. The loess RM, GBW07408a, showed a low CIA value (50.3) and a $\delta^{146/144}$Nd value (-0.010 ± 0.017 ‰, (2*s*, n = 3)) similar to that of BSE (-0.024 ± 0.031‰ (2*s*, n = 80) (McCoy-West *et al.* 2017, 2020a, 2021)), which could reflect the stable Nd isotopic ratios of the protolith in the weak chemical weathering stage. The limestone-forming soil

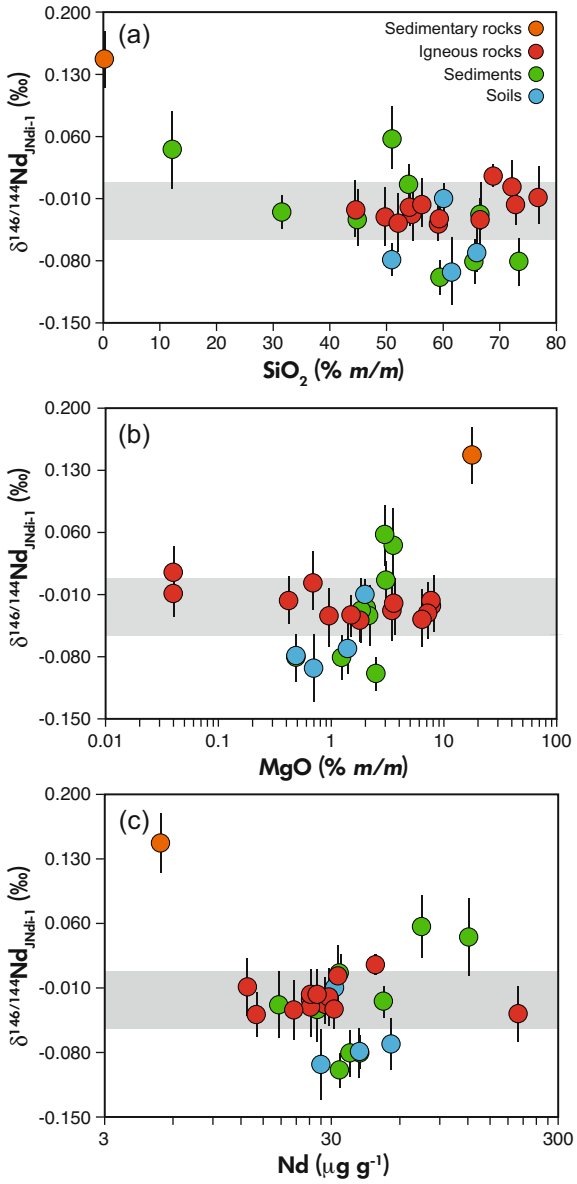

Figure 4. Stable Nd isotopic ratios versus SiO_2 (% *m/m*), MgO (% *m/m*), and Nd (μg g^{-1}) in these RMs measured in this study. Horizontal grey area represents the $\delta^{146/144}$Nd value of BSE with -0.024 ± 0.031‰ (2*s*, *n* = 80) taken from McCoy-West *et al.* (2021). Red circles are $\delta^{146/144}$Nd values of igneous rocks, green circles are values of sediments, blues are soil, and brown is dolomite. Range bars represent 2*s*. Data are taken from Table 1.

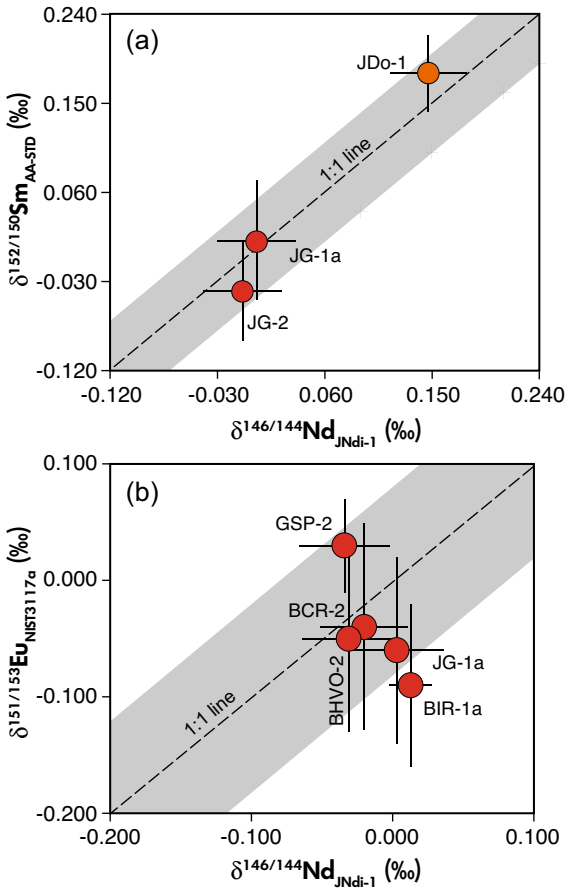

Figure 5. $\delta^{146/144}$Nd values obtained in this study versus available (a) $\delta^{152/150}$Sm and (b) $\delta^{151/153}$Eu values reported in the literature. Stable Sm and Eu isotopic data for these RMs were taken from Wakaki and Tanaka (2016) and Lee and Tanaka (2019), respectively. Dashed lines represent 1:1, with the shaded fields representing the reproducibility on $\delta^{152/150}$Sm of 0.05‰ and $\delta^{151/153}$Eu of 0.08‰, respectively. Range bars represent 2*s*.

(GBW07404a) and yellow-red soil (GBW07405a) both showed high CIA (94.4 and 92.7, respectively) and low $\delta^{146/144}$Nd values (-0.079 ± 0.018‰ (2*s*, *n* = 3) and -0.093 ± 0.038‰ (2*s*, *n* = 3), respectively), indicating that heavy Nd isotopes were preferentially leached from the soils during chemical weathering, similar to that with Ba isotopes (An *et al.* 2019). An *et al.* (2019) also measured a lateritic soil (GBW07407), and found that it has high CIA (97.9) and low $\delta^{138/134}$Ba values (-0.09 ± 0.05‰, 2*s*, *n* = 4). However, the yellow-red soil (GBW07405), which is of the same type as GBW07405a, showed a $\delta^{138/134}$Ba value (-0.03 ± 0.02 ‰, 2*s*, *n* = 2) to that of the upper continental crust of 0.00 ± 0.03‰ (2*s*, *n* = 71) (Nan *et al.* 2018), demonstrating that the fractionation mechanisms for stable Nd and Ba isotopes in soils are not identical. Although the chestnut soil (GBW07402a) from the giant Bayan Obo REE-Nb-Fe ore deposit district had a low CIA value (55.8), its $\delta^{146/144}$Nd value (-0.071 ± 0.028‰, (2*s*, *n* = 3)) remained lower than that of BSE (-0.024 ± 0.031‰, (2*s*, *n* = 80) McCoy-West *et al.* 2017, 2020a, 2021). This result

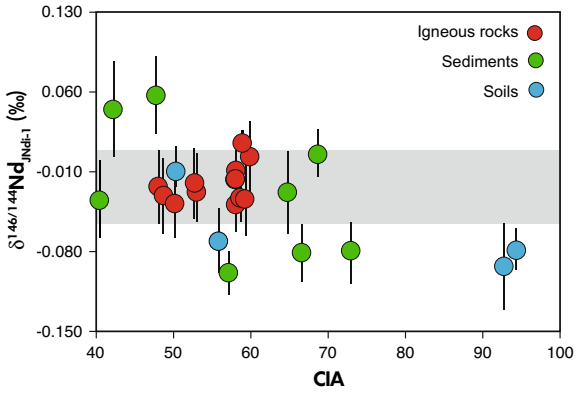

Figure 6. Stable Nd isotopic compositions versus CIA for RMs measured in this study. CIA = $A_2O_3/(A_2O_3 + CaO^* + Na_2O + K_2O)$ (where CaO* is amount of CaO in silicate phases only). The legend is same as that for Figure 4. $\delta^{146/144}$Nd values for soils and sediments were roughly negative with the degree of chemical weathering.

indicates that the stable Nd isotopic variations observed in the natural soils resulted from more than weathering process alone. Hence, additional investigations on the fractionation mechanisms of stable Nd isotopes in low-temperature geochemistry are required in the near future.

The dolomite RM (JDo-1) had the heaviest $\delta^{146/144}$Nd values (+0.147 ± 0.032‰, (2*s*, *n* = 3)), which was consistent with the $\delta^{146/144}$Nd values (+0.150 ± 0.040‰, 2*s*) measured by Ohno and Hirata (2013). The large stable Nd isotopic variations observed in this sample suggest that the sable Nd isotopes can become promising geochemical tracers to constrain the low-temperature sedimentary processes (Ohno and Hirata 2013). Similarly, the stable Sm isotopic ratio of JDo-1 reported by Wakaki and Tanaka (2016) showed significant isotopic fractionation. Therefore, combined studies of stable REEs isotopic systematics such as Nd, Sm and Eu may provide a significant advantage in elucidating low-temperature carbonate precipitation processes.

Conclusions

We present a comprehensive set of stable Nd isotopic data for twenty-seven geological RMs, including igneous rocks, river/marine sediments, soils and sedimentary rocks. The $\delta^{146/144}$Nd values of low-silica igneous rocks (SiO_2 < 70% *m/m*) had a very restricted range at -0.026 ± 0.020‰ (2s, *n* = 9), which was similar to those of BSE (-0.024 ± 0.031‰, (2s, *n* = 80)) and chondrites (-0.027 ± 0.026‰, (2s, *n* = 39)). The high-silica igneous rocks (SiO_2 > 70% *m/m*) have slightly higher $\delta^{146/144}$Nd values (-0.002 ± 0.028‰, 2s, *n* = 4) than that of BSE. The sediment samples have $\delta^{146/144}$Nd values ranging from -0.099‰ in GBW07335 to +0.057‰ in GBW07315, possibly reflecting the changes in the relative contributions of the different Nd sources. The soil RMs also show $\delta^{146/144}$Nd values ranging from -0.093‰ to -0.010‰, indicating that large stable Nd isotopic fractionation may occur during soil formations. The dolomite RM shows the heaviest $\delta^{146/144}$Nd value at +0.147 ± 0.032‰ (2*s*, *n* = 3), which is possibly ascribable to low-temperature carbonate precipitation. These data allow for a better understanding of the behaviour of the Nd in high-temperature magmatic processes to low-temperature chemical weathering. In addition, they can help in inter-laboratory comparisons and the quality assessment of data for stable Nd isotopic analyses in the future.

Acknowledgements

This research was financially supported by the Fundamental and Applied Fundamental Research Major Program of Guangdong Province (grant no. 2019B030302013), National Natural Science Foundation of China (grant no. 41991325, 42021002), Project of Science and Technology Development of Guangdong Academy of Sciences (grant no. 2019GDASYL-0301002), Key Special Project for Introduced Talents Team of Southern Marine Science and Engineering Guangdong Laboratory (Guangzhou) (grant no. GML2019ZD0308). We are grateful to the two anonymous reviewers for constructive comments and Dr. Christophe Quétel for editorial handing. We also appreciate Lei Zhang, Xianglin Tu, Shenglin Sun, and Yafei Xia for helpful isotopic analysis and Wiley at http://wileyeditingservices.com for English polishing. This is contribution No. IS-3213 from GIG-CAS.

Data availability statement

The data that support the findings of this study are available from the corresponding author upon reasonable request.

References

An Y.J., Li X. and Zhang Z.F. (2019)
Barium isotopic compositions in thirty-four geological reference materials analysed by MC-ICP-MS.
Geostandards and Geoanalytical Research, 44, 183–199.

references

Bai J.H., Liu F., Zhang Z.F., Ma J.L., Zhang L., Liu Y.F., Zhong S.X. and Wei G.J. (2021)
Simultaneous measurement stable and radiogenic Nd isotopic compositions by MC-ICP-MC with a single-step chromatographic extraction technique. Journal of Analytical Atomic Spectrometry, 36, 2695–2703.

Bothamy N. and Galy A. (2021)
Industrially purified Nd materials identified by distinct mass-dependent isotopic composition. Frontiers in environmental Chemistry.

Feng L.P., Zhou L., Yang L., DePaolo D.J., Tong S.Y., Liu Y.S., Owens T.L. and Gao S. (2017)
Calcium isotopic compositions of sixteen USGS reference materials. Geostandards and Geoanalytical Research, 41, 93–106.

He Y.S., Ke S., Teng F.Z., Wang T.C., Wu H.J., Lu Y.H. and Li S.G. (2015)
High-precision iron isotope analysis of geological reference materials by high-resolution MC-ICP-MS. Geostandards and Geoanalytical Research, 39, 341–356.

Inglis E.C., Moynier F., Creech J., Deng Z., Day J.M.D., Teng F.-Z., Bizzarro M., Jackson M. and Savage P. (2019)
Isotopic fractionation of zirconium during magmatic differentiation and the stable isotope composition of the silicate Earth. Geochimica et Cosmochimica Acta, 250, 311–323.

Lee S.-G. and Tanaka T. (2019)
Determination of Eu isotopic ratio by multi-collector inductively coupled plasma mass spectrometry using a Sm internal standard. Spectrochimica Acta Part B, 156, 42–50.

Liu F., Zhu H.L., Li X., Wang G.Q. and Zhang Z.F. (2017)
Calcium isotopic fractionation and compositions of geochemical reference materials. Geostandards and Geoanalytical Research, 41, 675–688.

Liu X., Wei G.J., Zou J.Q., Guo Y.R., Ma J.L., Chen X.F., Liu Y., Chen J.F., Li H.L. and Zeng T. (2018)
Elemental and Sr-Nd isotope geochemistry of sinking particles in the northern South China Sea: Implications for provenance and transportation. Journal of Geophysical Research: Oceans, 123, 9137–9155.

Ma J.L., Wei G.J., Liu Y., Ren Z.Y., Xu Y.G. and Yang Y.H. (2013)
Precise measurement of stable neodymium isotopes of geological materials by using MC-ICP-MS. Journal of Analytical Atomic Spectrometry, 28, 1926–1931.

McCoy-West A.J., Burton K.W., Millet M.-A. and Cawood P.A. (2021)
The chondritic neodymium stable isotope composition of the Earth inferred from mid-ocean ridge, ocean island and arc basalts. Geochimica et Cosmochimica Acta, 293, 575–597.

McCoy-West A.J., Chowdhury P., Burton K.W., Sossi P., Nowell G.M., Fitton J.G., Kerr A.C., Cawood P.A. and Williams H.M. (2019)
Extensive crustal extraction in Earth's early history inferred from molybdenum isotopes. Nature Geoscience, 12, 946–951.

McCoy-West A.J., Millet M.-A. and Burton K.W. (2017)
The neodymium stable isotope composition of the silicate Earth and chondrites. Earth and Planetary Science Letters, 480, 121–132.

McCoy-West A.J., Millet M.-A. and Burton K.W. (2020b)
The neodymium stable isotope composition of the oceanic crust: Reconciling the mismatch between erupted mid-ocean ridge basalts and lower crustal gabbros. Frontiers in Earth Science, 8.

McCoy-West A.J., Millet M.-A., Nowell G.M., Nebel O. and Burton K.W. (2020a)
Simultaneous measurement of neodymium stable and radiogenic isotopes from a single aliquot using a double spike. Journal of Analytical Atomic Spectrometry, 35, 388–402.

McCoy-West A.J., Mortimer N., Burton K.W., Ireland T.R. and Cawood P.A. (2022)
Re-initiation of plutonism at the Gondwana margin after a magmatic hiatus: The bimodal Permian-Triassic Longwood Suite, New Zealand. Gondwana Research, 105, 432–449.

Nakada R., Asakura N. and Nagaishi K. (2019)
Examination of analytical conditions of cerium (Ce) isotope and stable isotope ratio of Ce in geochemical standards. Geochemical Journal, 53, 293–304.

Nan X.Y., Yu H.M., Rudnick R.L., Gaschnig R.M., Xu J., Li W.Y., Zhang Q., Jin Z.D., Li X.H. and Huang F. (2018)
Barium isotopic composition of the upper continental crust. Geochimica et Cosmochimica Acta, 233, 33–49.

Nesbitt H.W. and Young G.M. (1982)
Early Proterozoic climates and plate motions inferred from major element chemistry of lutites. Nature, 299, 715–717.

Ohno T. and Hirata T. (2013)
Determination of mass-dependent isotopic fractionation of cerium and neodymium in geochemical samples by MC-ICPMS. Analytical Sciences, 29, 47–53.

Saji N.S., Wielandt D., Paton C. and Bizzarro M. (2016)
Ultra-high-precision Nd-isotope measurements of geological materials by MC-ICP-MS. Journal of Analytical Atomic Spectrometry, 31, 1490–1504.

Teng F.Z., Li W.Y., Ke S., Yang W., Liu S.A., Sedaghatpour F., Wang S.J., Huang K.J., Hu Y., Ling M.X., Xiao Y., Liu X.M., Li X.W., Gu H.O., Sio C.K., Wallace D.A., Su B.X., Zhao L., Chamberlin J., Harrington M. and Brewer A. (2015)
Magnesium isotopic compositions of international geological reference materials. Geostandards and Geoanalytical Research, 39, 329–339.

references

Wakaki S. and Tanaka T. (2012)
Stable isotope analysis of Nd by double spike thermal ionization mass spectrometry. International Journal of Mass Spectrometry, 323/324, 45–54.

Wakaki S. and Tanaka T. (2016)
Stable Sm isotopic analysis of terrestrial rock samples by double-spike thermal ionization mass spectrometry. International Journal of Mass Spectrometry, 407, 22–28.

Wang Y., Huang X., Sun Y., Zhao S. and Yue Y. (2017)
A new method for the separation of LREEs in geological materials using a single TODGA resin column and its application to the determination of Nd isotope compositions by MC-ICPMS. Analytical Methods, 9, 3531–3540.

Willig M. and Stracke A. (2018)
Accurate and precise measurement of Ce isotope ratios by thermal ionization mass spectrometry (TIMS). Chemical Geology, 476, 119–129.

Zhao P.P., Li J., Zhang L., Wang Z.B., Kong D.X., Ma J.L., Wei G.J. and Xu J.F. (2016)
Molybdenum mass fractions and isotopic compositions of international geological reference materials. Geostandards and Geoanalytical Research, 40, 217–226.

Zhu G., Ma J., Wei G. and Zhang L. (2021)
Boron mass fractions and $\delta^{11}B$ values of eighteen international geological reference materials. Geostandards and Geoanalytical Research.

Zhu H.L., Zhang Z.F., Wang G.Q., Liu Y.F., Liu F., Li X. and Sun W.D. (2016)
Calcium isotopic fractionation during ion-exchange column chemistry and thermal ionisation mass spectrometry (TIMS) determination. Geostandards and Geoanalytical Research, 40, 185–194.

Supporting information

The following supporting information may be found in the online version of this article:

Table S1. Detailed information on the reference materials analysed in this study.

Table S2. The major and trace element mass fractions in 100 ng g^{-1} Nd purified solutions through the Nd separation technique established here.

This material is available from: http://onlinelibrary.wiley.com/doi/10.1111/ggr.12451/abstract (This link will takeyou to the article abstract).